

# A Novel Cryo-SEM Technique for Imaging Vegetable Oil Based Organogels

Michael A. Rogers · Alexandra K. Smith ·  
Amanda J. Wright · Alejandro G. Marangoni

Received: 29 June 2007 / Revised: 8 August 2007 / Accepted: 10 August 2007 / Published online: 6 September 2007  
© AOCS 2007

**Abstract** Gels were prepared by cooling dilute solutions (2% wt/wt) of 12-hydroxystearic acid (12-HSA) in canola oil and storing them at 30 °C for 24 h. The gel's in-situ supramolecular network structure was imaged using four techniques: polarized light microscopy (PLM), 3-dimensional deconvolution polarized light microscopy (3DPLM), and cryo-scanning electron microscopy (cryo-SEM) of the xerogel and of an osmium tetroxide vapor fixed gel washed with isobutanol. Most of the canola oil was immobilized in the gel by fixation with osmium tetroxide therefore very little of the canola oil was removed during washing unlike the xerogel where all of the canola oil has been displaced. The in-situ supramolecular network structure as observed by PLM, was comparable to that seen through the new cryo-SEM method for fixed organogel. Cryo-SEM images of the xerogel did not show similar length scales or strand thickness as compared to the PLM images. The lengths of the network strands were much shorter for the xerogel as compared to the osmium tetroxide treated sample and the structures visualized by PLM. Furthermore, the thickness of the strands observed using PLM or cryo-SEM were in the size range of 3–10  $\mu\text{m}$  while the xerogels had strands in the range of 0.01–0.1  $\mu\text{m}$  thick. Therefore, the removal of canola oil from the gel using 80/20% v/v hexane/acetone with no fixation disrupted the supramolecular network.

## Introduction

Organogel formation and its application has attracted a great deal of research attention over the past 15 years. Recently, the rate of publication focusing on organogels has increased steadily [1]. Interest in these complex systems stems from their abundant applications in foods, pharmaceuticals, cosmetics and petrochemicals. However, the interest in “self-assembled fibrillar networks” (SAFINs) extends beyond food and pharmaceutical research. Many SAFINs are present in nature and include materials such as fibrous actin [2], clathrin [3], tubulin [4], keratin [5], insulin [6], collagen [7], silk [8], and amyloid fibrils which are associated with Alzheimer's and other neurodegenerative diseases [9]. In these systems, as the gelator is cooled in solution it forms a super-saturated solution and microscopic phase separation occurs rather than crystallization events which entail macroscopic phase separation. These gelator molecules self-assemble in stochastic nucleation events with highly specific interactions promoting one-dimensional growth [1].

Molecular gels require small molecular weight gelators to self-assemble prior to supramolecular aggregation of these structures. The formation of SAFINs occurs when the solution or sol is cooled below its gelation temperature. In terms of a molecular gel, the sol is defined as a dispersion of solid particles in a colloidal solution. Generally, the concentration of the gelator molecule is below 2 wt% which represents the percolation concentration threshold for fibrillar species under quiescent conditions [1].

As the solution is cooled below the melting point of the 12HSA gelator molecule it forms a super-saturated solution causing the gelator molecules to self-assemble via stochastic nucleation [1]. This one-dimensional growth results in fiber formation which may be described as ‘crystal-like’

M. A. Rogers · A. K. Smith · A. G. Marangoni (✉)  
Department of Food Science, University of Guelph,  
Guelph, ON, Canada N1G2W1  
e-mail: amarango@uoguelph.ca

A. J. Wright  
Department of Human Health & Nutritional Science,  
University of Guelph, Guelph, ON, Canada N1G2W1

[10]. SAFINs serve the same function as polymer chains in a polymer gel [10]. The junction zones and branching between these polymer-like SAFIN strands are responsible for the rigidity of the networks that form [10].

SAFINs self assemble via non-covalent bonds. The junction zones which form the supramolecular structure are also based on non-covalent interactions. SAFINs create a three-dimensional network structure by self-organizing via non-covalent interactions including: hydrogen bonding, van der Waals interactions,  $\pi$ - $\pi$  stacking, and metal coordination [11]. 12HSA canola oil gels the two predominate forces include hydrogen bonding and van der Waals forces. The interactions are strongly influenced by the nature of the liquid portion of the gel which promotes or discourages interactions among SAFINs. Although the many SAFINs are organogels (i.e. gels based on oil) there are examples of SAFINs which are hydrogels (i.e. gel based on water). The ability for SAFINs to self-assemble into rod-like structures is not well understood. It requires a balance between opposing parameters such as solubility in the solvent and those parameters which control epitaxial growth into axially symmetric elongated aggregates [1].

For gelation to occur in an organic solvent, both the self-assembly of the gelator molecules into fibers and the creation of three-dimensional network structures are required. Formation of fibers occurs via hydrogen bonding and the formation of the three-dimensional network occurs predominately via van der Waals interaction which has been demonstrated with L-lysine type organogelators [11].

Currently, cryogenic-temperature transmission electron microscopy (cryo-TEM) is the method of choice for imaging organogels due to the high resolution images [12]. The direct images can elucidate information regarding the basic building blocks of structures. However, cryo-TEM is limited to a sample thickness of approximately 300 nm. As well, it is not always possible to determine the interactions between strands by cryo-TEM because it is difficult to discern if the strands are on the same focal plane.

In the case of molecular gels, rheological properties result from supramolecular aggregates and their interactions with other strands [12]. In a recent study with 12HSA, the degree of dipole-dipole interactions in the solvent was proposed to determine the network structure [13]. In 12HSA organogels, fibrillar aggregates form crystalline nodes of different shapes depending on the solvent and gelator concentration [14]. For example, the supramolecular structure of 12HSA in cyclohexane varied from ribbon-like fibers to cylindrical fibers to lamellae, depending on the content of lecithin added to the sample [13]. This changed the appearance of the gel from turbid to translucent. Another interesting SEM study of 12HSA showed that, depending on if the D, L isomer or a racemic mixture was present, the physical appearance of the gels changed remarkably [15]. It

appears, depending on the isomer used to produce the gel, that the molecule twists in different directions; the authors found no twist in the racemic mixture of the gelator [15]. Two later studies suggest that the racemic mixture of 12HSA should produce platelets instead of fibers [16, 17]. Uzu and Sugiura [16] found that platelets were formed only when the D/L ratio was one. More recent work by Terech, Rodriguez, Barns and McKenna [18] found no major differences between the gel forming ability of the pure enantiomer and the racemic mixture. This study also found that 12HSA/benzene gels are more transparent than 12HSA in cyclohexane, nitrobenzene or hexafluorobenzene [18]. Therefore, the solvent influences network structure and extrapolation from a pure 12HSA/volatile solvent gel to the case of 12HSA/vegetable oil gels is not trivial.

Commonly, xerogels prepared for imaging are produced by the removal of all liquid oil prior to imaging. However, many gels made from low molecular weight organogelators (LMOGs) are polymorphous and undergo phase transitions during the removal of solvent [1]. In addition, during solvent removal gels may collapse onto themselves making it difficult to discern the supramolecular structure. SEM images were acquired for the 12HSA/soybean oil gels after complete solvent extraction using a mixed solvent (*n*-hexane/acetone = 8:2, v/v) [19]. A small portion of the gel was dispersed into the solvent overnight at room temperature. The gel, dispersed in the solvent, was added dropwise to a clean glass plate where it was dried and washed 10 times with the original solvent [19]. The residue was then coated with gold (ca. 30 nm). Using this technique 12HSA/soybean oil gels formed 0.01–0.1  $\mu\text{m}$  thick twisted fibers and each fiber had junction zones [19]. While this technique was useful because it illustrated the twisted fiber and some degree of branching, it is difficult to assume that no polymorphic transitions occurred during solvent removal or that the network junction zones were unchanged when the vegetable oil was extracted. Also, there is no reassurance that the network did not collapse onto itself. These factors make it very difficult to assume that the images acquired represent the in-situ network structure. The purpose of the present study was to develop an imaging technique suitable for visualizing 12HSA-vegetable oil based organogels, taking into consideration the challenges described above.

## Experimental

### Materials and Sample Preparation

A total of 99% pure DL-12HSA was obtained from Sigma-Aldrich (Catalogue Number 219967, St. Louis, MO, USA). The melting temperature of 12HSA was determined to be

76 °C using differential scanning calorimetry (Q2000, TA Instruments, New Castle, DE, US). Canola oil was obtained from Sunfresh Limited (batch 286G-C, Toronto, ON, CA) and used as received. 2wt% samples of 12HSA in canola oil were prepared by heating the 12HSA in canola oil to 85 °C for 30 min. The samples were then stored at 30 °C for 24 h in a Sanyo MIR-153 incubator (Sanyo Incubator, Japan) prior to image analysis to ensure that adequate time was given to anneal the network giving maximum structure.

## 2-Dimensional Polarized Light Microscopy Sample Preparation

Samples for thin film PLM were removed and stored in 30-mL glass containers (Fisher Scientific, Pittsburgh, PA, USA). After 24 h, a small portion of the gel was removed from the glass container and placed on a 25 × 75 × 1 mm glass slide (Fisher Scientific, Pittsburgh, PA, USA). A 22 × 22 × 0.15 mm glass cover slip (Fisher Scientific, Pittsburgh, PA, USA) was placed on top of the gel and compressed. The slide was then transferred into a thermostatically (30 °C) controlled microscope stage (Model LTS 350, Linkam Scientific, Surrey, UK) until analysis. Images were obtained using an Olympus BH polarized light microscope (Olympus, Tokyo, Japan) and a Sony XC-75 CCD video camera (Sony Corporation, Tokyo, Japan). Images were digitized using Scion Image Software (Scion Corporation, Fredrick, MD, USA) and were acquired using a 16-frame averaging method which resulted in an 8-bit grayscale image with a spatial resolution of 640 × 480 pixels. A 10× magnification objective lens with a 0.25 numerical aperture was used (Olympus, Tokyo, Japan).

## 3-Dimensional Deconvolution Polarized Light Microscopy Sample Preparation

A glass slide was used as the base and two glass coverslips were glued to the base using 2-part epoxy to create a small well in which to add the liquid sample (Fig. 1). The sample was added drop-wise in the molten state and a third coverslip was placed on top of the sample. The sample was then placed in the incubator at 30 °C and stored for 24 h. Samples were then imaged on a Leica microscope using polarized light (Leica Microsystems: DM-RXA2/CTR-MIC, Richmond Hill, ON, Canada). The polarizer was set to full extinction (90° relative to the analyzer). The 40× objective lens had a numerical aperture of 0.85. The images were collected using a cooled CCD camera (Q-Imaging: Retiga 1300, Burnaby, BC, Canada). Focused images were acquired as uncompressed 8-bit (256 greys) grayscale TIFF files with a 1,280 × 1,024 spatial resolution.

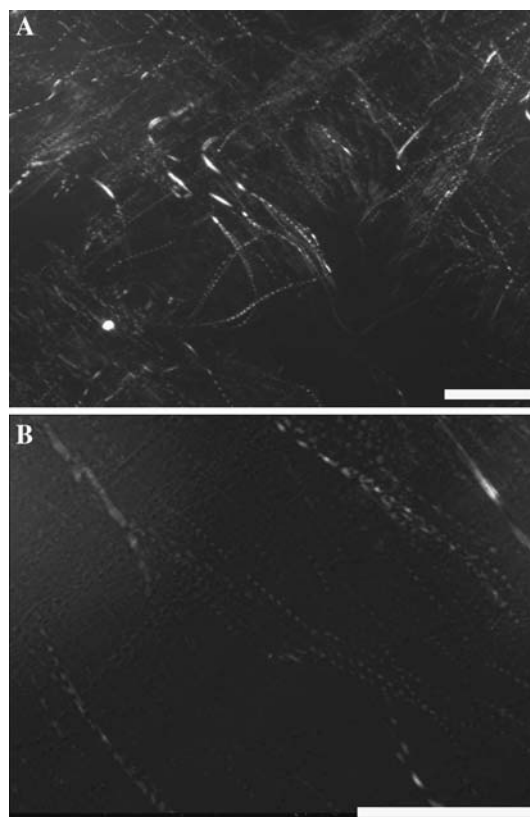


**Fig. 1** 2-Dimensional cross polarized light microscopy of 2%HSA/Canola oil; wt/wt under 10× magnification (a) and 40× magnification (b). Magnification Bar = 100 μm

Imaging was performed with the Openlab software module (Improvision Software and Scientific Imaging Inc, UK). This software included an automation allowing the user to input the following parameters: stage position at the top and bottom imaging planes, as well as number of optical slices desired between the two stage heights. Forty images were acquired from 80 μm through 170 μm from the sample. Upon completion of the z-series acquisition, the entire data set was saved in Openlab's proprietary "LIFF" file format. This file format saves all the images and layer information in one file.

The stack of images were then deconvolved using a "multiple neighbors" technique though Openlab 3.1.4 (Improvision Software and Scientific Imaging Inc, UK) and distributed by Quorum Technologies (Quorum Technologies Inc, Guelph, CA). The "multiple neighbors" technique uses a theoretical point spread function to perform the deconvolution [20, 21].

## Cryo-Scanning Electron Microscopy of 12HSA Xerogels

A drop of molten fat was placed on a glass coverslip which was coated with 30 nm of gold (Emscope K550 sputter

coater, Ashford, Kent, UK) and stored at 30 °C for 24 h after which time the coverslip was removed and 5 mL of 8:2 v/v *n*-hexane/acetone was applied dropwise to the surface of the fat in order to remove the canola oil from the matrix. The *n*-hexane/acetone was then washed from the surface with acetone which was allowed to volatilize at 30 °C.

The cover slip was mounted on a copper holder designed for the Emitech K550 Cryo-preparation unit (Ashford, Kent, UK) using Tissue-Tek<sup>®</sup>. The copper holder was plunged into a liquid nitrogen slush (−207 °C) which was prepared by pulling a vacuum on the liquid nitrogen. Liquid nitrogen slush provides a faster freezing rate than liquid nitrogen because the vapor barrier that forms at the surface of the sample is reduced (Leidenfrost phenomenon).

The copper holder was withdrawn from the freezing chamber through argon to prevent frost from forming on the surface of the samples. Once in the transfer device, the samples were put under vacuum. They were transferred, frozen and under vacuum, into the preparation chamber of the cryo-unit where the sample was sublimated at −80 °C for 30 min. The sample was then coated with 30 nm of gold (Emscope K1250x cryo-preparation system, Ashford, Kent, UK).

The holders were then transferred, frozen and under vacuum, onto the SEM (Hitachi S-570, Tokyo, Japan) cold stage which is held at −137 °C. Images were captured digitally using the Quartz PCI imaging software (Quartz Imaging Corp. Vancouver, BC).

### Cryo-Scanning Electron Microscopy of 12HSA/Canola Oil Gels

A drop of molten fat was placed on to a gold coated glass coverslip and stored at 30 °C for 24 h. The sample was then placed in a sealed metal container with 0.25 g osmium tetroxide (99.5% pure, Fisher Scientific, Pittsburgh, PA) to fix the unsaturated fatty acids in the canola oil. Once the oil had been fixed with osmium tetroxide vapors for 1 week at 30 °C the sample was removed and treated with different volumes of isobutanol in order to remove unfixed surface oil and to expose the supramolecular network structure. The glass coverslip was then attached to the copper holder for the cryo system and sample preparation was followed as above.

## Results and Discussion

The crystalline 12HSA network is birefringent and thus may be observed in-situ using PLM with little sample

preparation as shown in Fig. 1. PLM has been used to examine the crystalline nature of ricinelaiddic acid-canola oil gels [22]. The strands have segmented areas of bright and dark zones which relates to the twisted nature of the 12HSA strands [15–18]. According to Fig. 1a, b the 12HSA strands are approximately 100 μm long and 2–6 μm wide using the calibration bar as the reference length. In contrast, Tamura, Suetake, Ohkubo and Ohbu's [19], used cryo-SEM of the xerogels, and reported that the strand thickness of 12HSA/soybean oil xerogels to be 0.01–0.1 μm. These small strands would not be resolved by using polarized light with a 10× magnification objective lens of the in-situ gels. The differences can be attributed to differences in the method of sample preparation, including effects related to the removal of oil in the formation of the xerogel. These authors dispersed a small piece of gel into an *n*-hexane/acetone solution and added the dispersed solution drop-wise onto a clean glass plate, subsequently washing it with the original *n*-hexane/acetone solution [19]. Although this method provides some fundamental information on the network structure, the images acquired would not seem to correspond to the supramolecular in-situ structure as observed using PLM in the present study.

With PLM it is not possible to discern the depth of the strands visualized or the interactions between strands. It is difficult to determine if strands branch and how junction zones are established because of the inability to determine the *z*-position of the strand. Two strands may appear as though they are interacting but may be on different planes. An attempt to overcome this inability to discern the interactions of strands on different levels was made using 3DPLM. In 3DPLM the field of focus progresses through the sample every 2 μm and, using a nearest neighbors technique, the out-of-focus blur can be deconvolved from the image. Figure 2 shows that, using this approach, the interactions between strands were more obvious.

After a series of images in the *z* direction were collected, the images were stacked using a minimum intensity projection (Adobe Photoshop<sup>®</sup>, San Jose, CA, USA). This takes away from the ability to discern the interactions between strands. However, other important information about the in-situ structure may be gained from these images. According to Fig. 3, the strands are in excess of 100 μm long and up to 6 μm thick. Also, the segmented birefringence indicates that the strands are twisted. Despite these observations, the polarized light micrographs do not provide any insights as to the appearance of the individual strands or about the interactions and branching of strands.

In an attempt to visualize the finer network structure, cryo-SEM was used. Tamura, Suetake, Ohkubo and Ohbu's method [19] was adapted; the solvent was completely removed from the organogel matrix using a hexane/acetone 80:20 v/v solution. Instead of dispersing the gel into the hexane/acetone



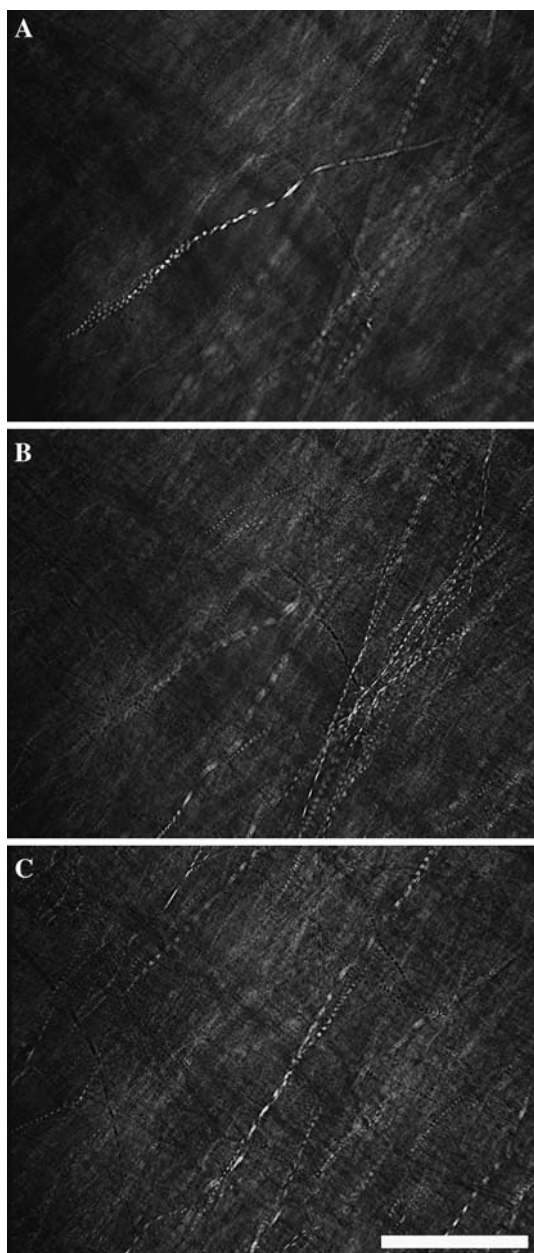


**Fig. 2** Micrographs of deconvolved images using the “nearest neighbors” technique, acquired using polarized light focused at the top (a), middle (b) and bottom (c) of the 170- $\mu\text{m}$  thick sample. *Magnification Bar = 100  $\mu\text{m}$*

solution, we attempted to preserve the supramolecular structure by dripping the solvent on the organogel matrix. When dispersing the gel matrix into the solvent, the network must be disrupted to become dispersed hence the supramolecular structure is most likely affected too. Once the network was deoiled, it was coated with gold and imaged. The longest structure in Fig. 4 was approximately 30  $\mu\text{m}$  long only a fraction of the 100  $\mu\text{m}$  structures observed by both PLM methods (Fig. 1–3). This indicates that the xerogel structure is dissimilar to the in-situ structure.

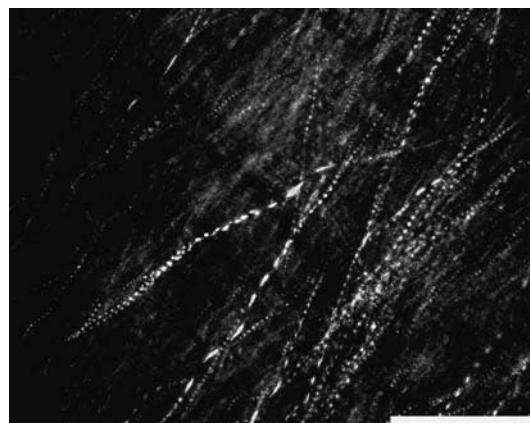


**Fig. 3** Micrographs of deconvolved images using the “nearest neighbors” technique acquired using polarized light microscopy and stacked using a minimum intensity projection of the individual slices from Fig. 2. *Magnification Bar = 100  $\mu\text{m}$*

Despite the drastic differences in structure between the PLM in-situ gels and the xerogels prepared by solvent deoiling, extremely valuable information on the self-assembling of the SAFINs can be obtained from the xerogel images. For example, the chiral mixture of the 12HSA forms a twisted helix in canola oil at 2%wt/wt which may be seen by the arrow in Fig. 4. Extensive branching is also evident. However, the solvent may have influenced the strands arrangements during deoiling. Sections of the 12HSA strands may have been displaced or broken and the stress of deoiling may have pulled the strands apart.

The invasive sample preparation has altered the structure therefore it is important to prepare the sample using a less

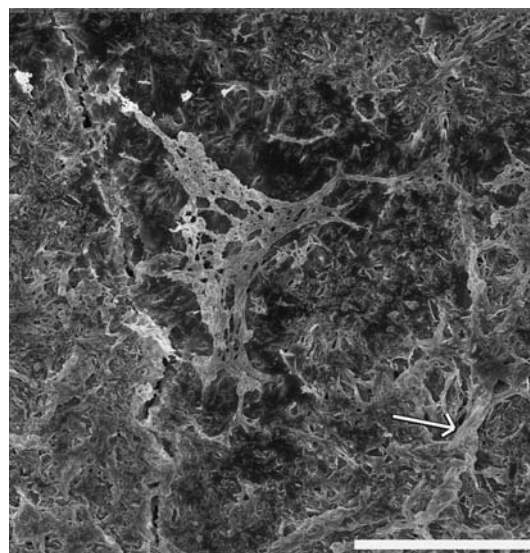


**Fig. 4** Cryo-SEM image of a xerogel of 12-HSA/Canola oil gel formed by removing the canola oil using a 80:20 *n*-hexane/acetone solution. *Magnification Bar = 30  $\mu\text{m}$*

**Fig. 5** Cryo-SEM of the osmium tetroxide vapor fixed gels with different degrees of isobutanol solvent washing. *Magnification Bar = 30 μm*

aggressive deoiling method. Therefore, the oil was removed from the 12HSA gels using a method similar to that of Chawla et al. [23]. The method was originally used to isolate fat crystals in margarines and shortenings. After the gel was stored at 30 °C for 24 h, the sample was exposed to osmium tetroxide vapors in order to fix the canola oil. The benefit of osmium fixation is that it stabilized the structure and it confers electron density to the specimen [24]. The osmium tetroxide binds to the unsaturated double bonds of fatty acids to form cross-links [25, 26]). Early work using osmium tetroxide showed that the application to fat crystals did not affect their morphology [27]. Since, 12HSA organogels are comprised of fatty acid networks made of crystallites, the application of osmium tetroxide should have a similar effect on the crystal morphology of the strands as it does on spherulitic fat crystals.

Figure 5 shows the supramolecular structure of the osmium tetroxide treated 12HSA/canola oil organogel. Without etching with isobutanol, very little network structure can be observed. When the sample was treated only with osmium, the surface oil covers the 12HSA network and very little information may be obtained. From the top image of Fig. 5a, we can observe that the length and thickness of the strands in the network are more similar to that shown in Figs. 1–3 which illustrates the in-situ structure of the 12HSA network. The length of the 12HSA strands in the osmium treated gel is in excess of 100 μm, as seen in the PLM and 3DPLM images. In the xerogels, the strands were a fraction of this. The osmium treated sample without a solvent wash clearly shows a 12HSA network in which strands branch into two smaller, individual strands. This imaging technique shows that individual strands originate from the same parent strand. This type of branching is due to a crystallographic mismatch which is based on a nucleation-growth-branching-growth-branching-growth modeled by Lui and Sawant [28]. However, without etching with isobutanol, surface characteristics are not easily observable nor can the amount of network structure present be determined. This shows that 12HSA networks do not form at the oil/air interface. Furthermore, the surface of the 12HSA network may be slightly affected by the chemical reaction between the vegetable oil and the osmium tetroxide. This may give rise to the smooth strand surface structure seen in the images. However, this method provides insight into how 12HSA strands branch and how they self-assemble into large supramolecular networks.

The dropwise application of isobutanol to the surface of the gel etches away the unfixed unsaturated oil which allows the 12HSA network to be exposed. Three different

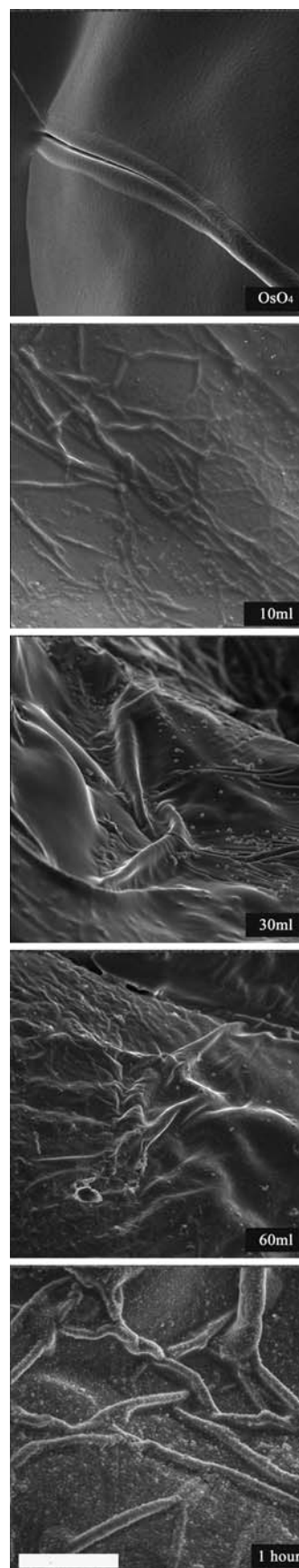




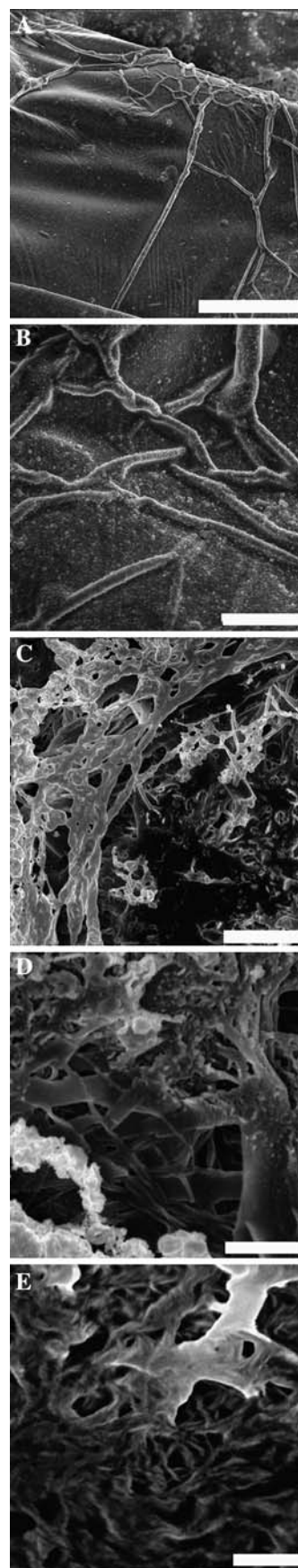
**Fig. 6** Cryo-SEM of 12HSA organogels imaged using osmium tetroxide fixation and isobutanol washing (**a** (Magnification bar = 100  $\mu\text{m}$ ), **b** (Magnification Bar = 30  $\mu\text{m}$ )) and of the xerogel produce by washing with a hexane/acetone solution (**c** (Magnification Bar = 6  $\mu\text{m}$ ), **d** (Magnification Bar = 2  $\mu\text{m}$ ), **e** (Magnification Bar = 1  $\mu\text{m}$ ))

quantities of isobutanol were added drop-wise to the gel: 10, 30 and 60 mL in order to observe if network collapse occurs during deoiling. Figure 5a shows that only a small amount of surface oil is being etched away, exposing a single layer of network structure. Observing these images (Fig. 5) with varying degrees of solvent washing demonstrates that there are several different strand thickness in the network. The network matrix is highly branched and the network strands interact by twisting themselves around other strands. Therefore, the network attains its structure not only from branching network strands but also because of strand entanglement. Since only a small amount of oil has been etched from the surface it does not appear that the network collapses onto itself. Furthermore, two different types of strands are present in the network: some in excess of 10  $\mu\text{m}$  thick and others which are less than 3  $\mu\text{m}$  thick. This is also observed in the PLM images where the 10- $\mu\text{m}$  strands correspond to the highly birefringent segmented strands and the thin 3  $\mu\text{m}$  strands are observed as the birefringent disordered network.

In order to test the effect of prolonged exposure to isobutanol, the sample was treated with osmium tetroxide and etched by soaking a small drop of gel on a glass slide in isobutanol. This sample was soaked for 1 h, removed carefully to ensure that the sample stayed adhered to the glass slide, and then rinsed with acetone. From this, it is apparent that the network structure is similar to the case when the isobutanol is added drop-wise. Hence, we can conclude that no significant collapse takes place during prolonged exposure to isobutanol.

Different levels of structure can be discerned in the 12HSA networks at different levels of magnification (Fig. 6). At the low magnifications (i.e. Fig. 6a and b, Bar = 100  $\mu\text{m}$  and Bar = 30  $\mu\text{m}$ , produced by treating the gel with osmium tetroxide and isobutanol) it is apparent that the network structure is highly organized with strands exceeding 200  $\mu\text{m}$  in length. The network appears to be highly branched and entangled which would give the network its viscoelastic properties. Also, these images show the void volume between the strands where canola oil was present in the gel. These large immobilized pockets within the network structure may be used to encapsulate enzymes or lipophilic bioactive compounds.

The xerogels prepared by complete deoiling of the samples (i.e. solvent mixture of hexane and acetone) are also shown at higher magnifications (Fig. 6, (c) Bar = 6  $\mu\text{m}$ , (d) Bar = 2  $\mu\text{m}$  and (e) Bar = 1  $\mu\text{m}$ ). According to



these images, the basic building blocks of the network are highly organized into a twisted helix that is highly branched. However, no structures thicker than 2  $\mu\text{m}$  are present in these images, although they are apparent in both the PLM images and the cryo-SEM images when treated with osmium tetroxide and isobutanol.

## Conclusion

Comparison of the cryo-SEM 12HSA xerogel, the osmium tetroxide isobutanol treated samples and the in-situ PLM images, we observed that the structural features are similar between the PLM images and the osmium tetroxide/isobutanol treated samples. Creation of a xerogel, using a traditional solvent extraction disrupts the in-situ supramolecular network structure altering the network and affecting the appearance (size and length) of the strands. Using osmium tetroxide-isobutanol sample preparation the network structure is more comparable to the in-situ structure observed using PLM. The method of application of the isobutanol to the sample does not appear to significantly change the amount of canola oil removed from the sample.

Treating the 12HSA/canola oil organogel with osmium tetroxide prior to washing with isobutanol greatly improves the ability to image and resolve the supramolecular network. Producing the xerogel prior to imaging also provides valuable information regarding the twist of the strands and how the building blocks self-assemble. However, to observe the supramolecular network structure, the chemically fixed network is more representative of the in-situ structure.

## References

- Weiss RG, Terech P (2006) Introduction. In: Weiss RG, Terech P (eds) *Molecular gels materials with self-assembled fibrillar networks*. Springer, Dordrecht, Netherlands, pp 1–13
- Greer SC (2002) Reversible polymerizations and aggregations. *Annu Rev Phys Chem* 53:173–200
- Kirchhausen T (2000) Clathrin. *Annu Rev Biochem* 69:699–727
- Oakley BR, Akkari YN (1999)  $\gamma$ -Tubulin at ten: progress and prospects. *Cell Struct Funct* 24:365–372
- Fuchs E (1995) Keratins and the skin. *Annu Rev Cell Dev Biol* 11:123–153
- Waugh DF (1946) A fibrous modification of insulin. I. The heat precipitate of insulin. *J Am Chem Soc* 68:247–250
- Caria A, Bixio L, Kostyuk O, Ruggiero C (2004) Elastic scattering and light transport in three-dimensional collagen gel constructs: a mathematical model and computer simulation approach. *IEEE Trans Nanobioscience* 3:85–89
- Jin H-J, Kaplan DL (2003) Mechanism of silk processing in insects and spiders. *Nature* 424:1057–1061
- Lui W, Prausnitz JM, Blanch HW (2004) Amyloid fibril formation by peptide LYS (11–36) in aqueous trifluoroethanol. *Biomacromolecules* 5:1818–1823
- Terech RG, Furman I, Weiss RG (1995) Structures of organogels based upon cholesteryl 4-(2-anthryloxy)butanone, a highly effective luminescing gelator: neutron and X-ray small-angle scattering investigations. *J Phys Chem* 99:9558–9566
- Suzuki M, Nakajima Y, Yumoto M, Kimura M, Shirai H, Hanabusa K (2003) Effects of hydrogen bonding and van der Waals interactions on organogelation using designed low-molecular weight gelators and gel formation at room temperature. *Langmuir* 19:8622–8624
- Danino D, Talmon Y (2006) Direct-imaging and freeze-fracture cryo-transmission electron microscopy of molecular gels. In: Weiss RG, Terech P (eds) *Molecular gels materials with self-assembled fibrillar networks*. Springer, Dordrecht, Netherlands, pp 253–275
- Tamura T, Ichikawa M (1997) Effect of lecithin on organogel formation of 12-hydroxystearic acid. *J Am Oil Chem Soc* 74:491–504
- Terech P (1992) 12-D-hydroxyoctadecanoic acid organogels: a small angle neutron scattering study. *J Phys II France* 2:2181–2195
- Tachibana T, Kambara H (1968) The sense of twist in the fibrous aggregates from 12-hydroxystearic acid and its alkali metal soaps. *J Colloid Interface Sci* 28:173–174
- Uzu Y, Sugiura T (1975) Electron microscopic and thermal studies of optically active 12-hydroxystearic acids in soap formation. *J Colloid Interface Sci* 51:346–349
- Fuhrhop J-H, Schnieder P, Rosenberg J, Boekema E (1987) The chiral bilayer effect stabilized micellar fibers. *J Am Chem Soc* 109:3387–2290
- Terech P, Rodrigues V, Barns JD, McKenna GB (1994) Organogels and aerogels of racemic chiral 12-hydroxystearic acid. *Langmuir* 10:3406–3418
- Tamura T, Suetake T, Ohkubo T, Ohbu K (1994) Effect of alkali metal ions on gel formation in the 12-hydroxystearic acid/soybean oil system. *J Am Chem Soc* 71:85–89
- McNally J, Karpova T, Cooper J, Conchello J (1999) Three-dimensional imaging by deconvolution microscopy. *Methods* 19:373–385
- Wallace W, Schaefer L, Swedlow J (2001) A working person's guide to deconvolution in light microscopy. *BioTechniques* 31(5):1–16
- Wright AJ, Marangoni AG (2007) Time, temperature and concentration dependence of ricinelaidic acid-canola oil organogelation. *J Am Oil Chem Soc* 84:3–9
- Chawla P, deMan JM, Smith AK (1990) Crystal morphology of shortenings and margarines. *Food Struct* 9:329–336
- Revel JP (1975) Elements of scanning electron microscopy for biologists. *Scan Electron Microsc*, 687–696
- Hayat MA (1970) Principles and techniques of electron microscopy: biological applications, vol 1. Van Nostrand Reinhold Co., New York, pp 39–44
- deMan JM, Mostafa AN, Smith AK (1985) Thermal analysis microscopy for the study of phase changes in fats. *Food Microstruct* 4:233–332
- Mostafa A, Smith AK, deMan JM (1985) Crystal structure of hydrogenated canola oil. *J Am Oil Chem Soc* 62:760–762
- Lui XY, Sawant PD (2002) Mechanism of the formation of self organized microstructures in soft functional materials. *Adv Mater* 14:421–426